Quantum effects in the quasiparticle structure of the ferromagnetic Kondo lattice model

2001 J. Phys.: Condens. Matter 13 2531

(http://iopscience.iop.org/0953-8984/13/11/310)

INSTITUTE OF PHYSICS PUBLISHING JOURNAL OF PHYSICS: CONDENSED MATTER

J. Phys.: Condens. Matter **13** (2001) 2531–2548 www.iop.org/Journals/cm PII: S0953-8984(01)19290-8

Quantum effects in the quasiparticle structure of the ferromagnetic Kondo lattice model

D Meyer[1], **C Santos and W Nolting**

Lehrstuhl Festkörpertheorie, Institut für Physik, Humboldt-Universität zu Berlin, Invalidenstraße 110, 10115 Berlin, Germany

Received 22 November 2000, in final form 31 January 2001

Abstract

A new 'dynamical mean-field theory' based approach for the *Kondo lattice model* with quantum spins is introduced. The inspection of exactly solvable limiting cases and several known approximation methods, namely the *second-order perturbation theory*, the *self-consistent CPA* and finally a *moment-conserving decoupling* of the equations of motion, help in evaluating the new approach. This comprehensive investigation gives some certainty to our results. Whereas our method is somewhat limited in the investigation of the $J < 0$ model, the results for $J > 0$ reveal important aspects of the physics of the model: the energetically lowest states are not completely spin-polarized. A band splitting, which occurs already for relatively low interaction strengths, can be related to distinct elementary excitations, namely magnon emission (absorption) and the formation of magnetic polarons. We demonstrate the properties of the ferromagnetic Kondo lattice model in terms of spectral densities and quasiparticle densities of states.

1. Introduction

The Kondo model and its periodic extension, the Kondo lattice model (KLM), which describes spin-exchange interaction between a localized spin or a system of localized spins, respectively, and a band of itinerant electrons, has been the subject of intense theoretical studies in the past [1–6]. This model has been applied to a variety of different problems in solid-state physics using both a ferromagnetic and antiferromagnetic coupling constant J.

The model with $J < 0$ is the one originally known as the *Kondo lattice model* or simply *Kondo model* in its non-periodic form with a single impurity spin in the system. It was used by Kondo to explain the unusual temperature behaviour of the resistivity of magnetic impurities in non-magnetic hosts [4]. The negative spin-exchange interaction can be derived from the hybridization of a correlated 'atomic' level with a conduction band, the situation described by the Anderson model [7, 8]. In the limit of a low-lying half-filled atomic level and strong correlations, the Anderson model can be mapped onto the Kondo model with a negative exchange constant [9]. The Kondo lattice model is still subject to much theoretical work, the

[1] Present address: Department of Mathematics, Imperial College, London, UK.

0953-8984/01/112531+18$30.00

main objective is the understanding of the unusual physical behaviour found in *heavy-fermion* materials [8].

A model with identical operator structure in the Hamiltonian, but with positive exchange constant has been known in the literature for a long time by many different names (double exchange model, s–d model, s–f model, etc) [1, 3, 5, 6]. For clarity, we will refer to this model in the following as the *ferromagnetic Kondo lattice model*. The model with ferromagnetic exchange has to be understood as an effective one. The origins of the exchange with $J > 0$ are found in the interband Coulomb correlations [3]. This situation is believed to dominate the physical properties of important systems such as the magnetic semiconductors [10] (EuX; X = O, S, Se, Te), the diluted magnetic semiconductors [11] ($Cd_{1-x}Mn_xTe$, $Hg_{1-x}Fe_xSe$), and the 'local moment' metals [12] (Gd, Dy, Tb). To these problems, the ferromagnetic KLM was successfully applied [13–15]. Recently, this variant of the KLM has gained a lot of interest with the discovery of the colossal magnetoresistance (CMR) materials [16, 17]. In these materials, typically manganese oxides with perovskite structure ($La_{1-x}(Ca,Sr)_xMnO_3$), the double-exchange model [1, 2] has been successfully applied to explain the origin of ferromagnetic order and is expected to be a good starting point to investigate the resistivity anomalies [18]. This double-exchange model, however, is nothing else than the Kondo lattice model with ferromagnetic (positive) exchange constant in the strong coupling limit. In the CMR materials, the localized $S = \frac{3}{2}$ spin of the model represents the more or less localized manganese 3d-t_{2g} electrons, whereas the conduction band is formed by the e_g electrons. The interband-exchange interaction is nothing else but the intra-shell Hund's rule coupling. Since the 3d-e_g electrons of the manganese form a relatively narrow band (theoretical results from band-structure calculations: 1–2 eV [19–21], and experimental estimates: 3–4 eV [22, 23]) and Hund's coupling is assumed to be large, the model has to be taken in the intermediate to strong coupling regime. There are a few estimates of the value of the interaction constant in the literature, e.g. $J \approx 1$ eV [19, 24], but these are challenged as being too small [25]. Most theoretical papers of the last few years concerned with colossal magnetoresistance assume classical spins $S \to \infty$ [26–29]. This has been justified by the assumption of $JS \to \infty$ [25]. Although it is true that the important energy scale is JS, there are many more implications of $S \to \infty$ that are not justified in the strong-coupling limit for a $S = \frac{3}{2}$ system. In several papers, it was stated that '... the e_g electrons are oriented parallel to the t_{2g} spins' [28] or equivalently '... so one only need consider configurations with e_g electrons parallel to core spins' [25]. We will show below using exact results as well as several well-defined approximation methods, that for $S = \frac{3}{2}$ there is a considerable amount of spin-$\downarrow$ spectral weight located in the main region of the spin-$\uparrow$ states even for large interaction strengths. The assumption of a half-metallic state [30], made in the two citations above can therefore never be met in the KLM with quantum spins and is merely an effect of the (unphysical) limit of 'classical' spins. The recently discussed half-metallic behaviour of the manganites [31] must have a different origin.

However, for the opposite sign of J, exactly the assumed effect happens in the strong-coupling limit: the lowest-lying excitations in the conduction band density of states will be purely spin-$\downarrow$. This already implies that results for the Kondo lattice model with $J > 0$ and $J < 0$ cannot simply be reverted into the respective other case. The change of sign changes the whole physics of the system. For $J < 0$ an antiparallel ('antiferromagnetic') alignment of the conduction band spin and the localized spin lowers the internal energy. For a sufficient band filling, this tends to a screening of the local moments by conduction electrons, well known from the Kondo effect that refers to a single magnetic impurity in a conduction electron sea. From this, the name 'Kondo lattice model' was originally derived for the $J < 0$ case.

We will further show that already for comparatively low interaction strengths the spin-exchange interaction alone leads to an opening of a gap in the density of states. This

extraordinary correlation effect could give hints to the explanation of a recently discovered pseudogap in the managese oxides [32].

To prove our claims already laid out so far, we will first review two important non-trivial exactly solvable limiting cases of the Kondo lattice model in section 2. The first is the *zero-bandwidth limit* ('atomic limit') where the bandwidth of the conduction band is set to $W = 0$ [33]. The second exactly solvable limiting case is the so-called *ferromagnetically saturated semiconductor* [13, 14, 34–42]. This is essentially the zero-temperature limit of the model with vanishing electron density and fully aligned spin system. In this limit, striking correlation effects can be observed and discussed. These limiting cases will already give clear evidence to our propositions made above. In section 3 we will present a new *dynamical mean-field theory* (DMFT)-based approach for the KLM with $S = \frac{1}{2}$ spins. To circumstantiate our theory, we will introduce three more approximation schemes which also keep the spin as a quantum variable, not relying on the classical spin limit. The first will be a *second-order perturbation theory* (SOPT) for the KLM based on the projector operator formalism [43, 44]. The *self-consistent CPA* (coherent potential approximation) is a straightforward extension to the well known CPA for the KLM [6, 45–48]. It starts from the zero-bandwidth limit discussed before. The third approximation method is a moment-conserving decoupling procedure for the equation of motion of the single-electron Green function. This approximation scheme continuously evolves from the exactly solvable limit of the ferromagnetically saturated semiconductor. It will be called the *moment-conserving decoupling approximation* (MCDA). The comparison of the results obtained by these three methods and our DMFT scheme, each of which starts from a different limit, allows us to evaluate the range of applicability of the new approach, and to select the most trustworthy common features of all methods to gain a reliable picture of the physics of the ferromagnetic KLM.

2. The Kondo lattice model and its many-body problem

2.1. Hamiltonian

The Kondo lattice model (or s–f model) traces back the characteristic features of the underlying physical system to an interband exchange coupling of itinerant conduction electrons to (quasi-) localized magnetic moments described by the following model Hamiltonian [5, 6]

$$H = H_s + H_{sf} + \left(H_U + H_{ff}\right)$$
$$= \sum_{ij\sigma} T_{ij} c^{\dagger}_{i\sigma} c_{j\sigma} - J \sum_{i} \sigma_i \cdot \boldsymbol{S}_i + \left(\frac{1}{2} U \sum_{i,\sigma} n_{i\sigma} n_{i-\sigma} - \sum_{i,j} \hat{J}_{ij} \boldsymbol{S}_i \cdot \boldsymbol{S}_j \right). \quad (1)$$

$c^{\dagger}_{i\sigma}$ ($= \frac{1}{\sqrt{N}} \sum_{\boldsymbol{k}} c^{\dagger}_{\boldsymbol{k}\sigma} \mathrm{e}^{-\mathrm{i}\boldsymbol{k}\cdot\boldsymbol{R}_i}$) and $c_{i\sigma}$ are, respectively, creation and annihilation operators of a band electron being specified by the lower indices. The hopping integrals T_{ij} are connected by Fourier transformation to the single-electron Bloch energies $T_{ij} = \frac{1}{N} \sum_{\boldsymbol{k}} \epsilon(\boldsymbol{k}) \mathrm{e}^{\mathrm{i}\boldsymbol{k}\cdot(\boldsymbol{R}_i - \boldsymbol{R}_j)}$.

The interband (sf) exchange with coupling strength J is taken as an intra-atomic interaction between the conduction electron spin σ_i and the localized magnetic moment represented by the spin operator $\boldsymbol{S}_i$. For practical reasons it is sometimes convenient to use the second quantization representation of the band electron spin σ_i which leads to the following form of the interband-interaction term:

$$H_{sf} = -\frac{1}{2} J \sum_{i,\sigma} \left(z_\sigma S^z_i n_{i\sigma} + S^{\sigma}_i c^{\dagger}_{i-\sigma} c_{i\sigma} \right). \quad (2)$$

Here we have used the abbreviations $n_{i\sigma} = c^{\dagger}_{i\sigma} c_{i\sigma}$, $z_{\uparrow(\downarrow)} = +1(-1)$ and $S^{\sigma}_i = S^x_i + \mathrm{i} z_\sigma S^y_i$. The first term in (2) describes an Ising-like interaction between the z-components of the spin

operators, while the second term incorporates spin exchange processes between the localized and the itinerant system.

The last two terms are an extension to the original model: H_U leads to the 'correlated Kondo lattice model', it introduces correlations between the conduction electrons in form of a 'Hubbard-type' interaction. We will include this term in some parts of the discussion below. The second term, H_{ff} represents a direct spin exchange between localized moments on different lattice sites. Although the sf exchange can lead to an effective RKKY interaction between the spins for non-vanishing band occupation, a 'superexchange' could also be included. In case of an empty conduction band, this term becomes essential as the source of magnetic order. $\hat{J}_{ij}$ are the superexchange integrals. We state once more that the original Kondo lattice model (or s–f model) is defined by $H = H_s + H_{sf}$ only. The additional terms in equation (1) are used as soon as physical requirements do not allow us to neglect them.

If we are mainly interested in the conduction electron properties then the single-electron Green function $G_{ij\sigma}(E) = \langle\langle c_{i\sigma}; c^{\dagger}_{j\sigma}\rangle\rangle_E$ is of primary interest. Its equation of motion reads for the correlated KLM

$$\sum_m (E\delta_{im} - T_{im})G_{mj\sigma}(E) = \hbar\delta_{ij} - \tfrac{1}{2}J\left(z_\sigma I_{ii,j\sigma}(E) + F_{ii,j\sigma}(E)\right) + U\Gamma_{iii,j\sigma}(E). \tag{3}$$

The two types of interaction terms in (2) let the 'spinflip function' $F_{im,j\sigma}(E) = \langle\langle S_i^{-\sigma} c_{m-\sigma}; c^{\dagger}_{j\sigma}\rangle\rangle_E$ and the 'Ising function' $I_{im,j\sigma}(E) = \langle\langle S_i^z c_{m\sigma}; c^{\dagger}_{j\sigma}\rangle\rangle_E$ appear, while the 'Hubbard-function' $\Gamma_{ilm,j\sigma}(E) = \langle\langle c^{\dagger}_{i-\sigma} c_{l-\sigma} c_{m\sigma}; c^{\dagger}_{j\sigma}\rangle\rangle_E$ comes into play only when the 'Hubbard-interaction' (the U-term in equation (1)) is switched on.

The three 'higher' Green functions on the right-hand side of equation (3) prevent a direct solution of the equation of motion. A formal solution for the Fourier-transformed single-electron Green function

$$G_{k\sigma}(E) = \langle\langle c_{k\sigma}; c^{\dagger}_{k\sigma}\rangle\rangle_E = \frac{\hbar}{E - \epsilon(k) - \Sigma_{k\sigma}(E)} \tag{4}$$

defines the electronic self-energy $\Sigma_{k\sigma}(E)$ by the ansatz $\langle\langle [c_{k\sigma}; H - H_s]_- ; c^{\dagger}_{k\sigma}\rangle\rangle_E = \Sigma_{k\sigma}(E) G_{k\sigma}(E)$. For the general case $\Sigma_{k\sigma}(E)$ cannot be determined rigorously.

Before introducing some approaches to the not exactly solvable many-body problem of the KLM let us discuss in the next sections two rather illustrative limiting cases which can help to test the unavoidable approximations.

2.2. The zero-bandwidth limit

Let us assume that the arbitrarily filled conduction band is shrunk to an N-fold degenerate level T_0: $\epsilon(k) \to T_0\ \forall k$. Nevertheless, we consider the f-spin system as collectively ordered for $T < T_c$ by any direct or indirect exchange interaction. In this case, the hierarchy of equations of motion decouples exactly and can rigorously be solved [33]. The resulting energies and respective spectral weights are

$$\begin{aligned}
E_1 &= T_0 - \tfrac{1}{2}JS & \alpha_{1\sigma} &= \frac{1}{2S+1}\{S + 1 + z_\sigma\langle S^z\rangle + \gamma_{-\sigma} \\
&&&\quad - z_\sigma\Delta_{-\sigma} - (S+1)\langle n_{-\sigma}\rangle\} \\
E_2 &= T_0 + \tfrac{1}{2}J(S+1) & \alpha_{2\sigma} &= \frac{1}{2S+1}\{S - z_\sigma\langle S^z\rangle - \gamma_{-\sigma} \\
&&&\quad + z_\sigma\Delta_{-\sigma} - S\langle n_{-\sigma}\rangle\} \\
E_3 &= T_0 + U - \tfrac{1}{2}J(S+1) & \alpha_{3\sigma} &= \frac{1}{2S+1}\{S\langle n_{-\sigma}\rangle - \gamma_{-\sigma} + z_\sigma\Delta_{-\sigma}\} \\
E_4 &= T_0 + U + \tfrac{1}{2}JS & \alpha_{4\sigma} &= \frac{1}{2S+1}\{(S+1)\langle n_{-\sigma}\rangle + \gamma_{-\sigma} - z_\sigma\Delta_{-\sigma}\}.
\end{aligned} \tag{5}$$

The 'Hubbard-U' in E_3 and E_4 indicates that these excitations are bound to a double occupancy of the respective lattice site. E_1 and E_2 appear when our 'test electron' enters an empty site. If it orients its spin parallel to the local f-spin then the energy E_1 is needed. In the case of an antiparallel spin orientation a triplet or a singlet state is formed. The first requires the energy E_1, the second E_2. The latter is therefore two-fold degenerate. The spectral weights are, contrary to the energy levels, strongly dependent on the magnetization state of the f system and the band filling. For a complete solution one needs the average occupation number $\langle n_{-\sigma}\rangle$ and the mixed correlation functions $\gamma_\sigma = \langle S_i^\sigma c_{i-\sigma}^\dagger c_{i\sigma}\rangle$ and $\Delta_\sigma = \langle S_i^z n_{i\sigma}\rangle$. The evaluation can self-consistently be done by use of the spectral theorem for the Green functions $G_{ii\sigma}(E)$, $I_{ii,i\sigma}(E)$ and $F_{ii,i\sigma}(E)$ (cf [33]). It is interesting to observe that in any case from the four poles only three appear. For less than half-filled bands and $J > 0$ ($J < 0$) $\alpha_{3\sigma}$ ($\alpha_{4\sigma}$) vanishes, and for more than half-filled $\alpha_{2\sigma}$ ($\alpha_{1\sigma}$) vanishes. It should be mentioned that the spectral weights $\alpha_{i\sigma}$ do not explicitly depend on the coupling constants J and U. That means, on the one hand, that even for $U = 0$ the s–f interaction produces a splitting into four non-coincident quasiparticle levels. On the other hand, there is a striking dependence of $\Delta_{-\sigma}$ and $\langle n_{-\sigma}\rangle$ on the sign of the s–f coupling. That transfers to the spectral weights giving them some indirect dependence on $J/|J|$. For $J > 0$ and $J < 0$ the order of the energy levels is different resulting via the spectral theorem in different correlation functions. Note that the mentioned dependence on J concerns only the sign of J. The spectral weights are not influenced by the absolute value $|J|$.

2.3. The ferromagnetically saturated semiconductor

There is another very instructive limiting case that can be treated rigorously. It concerns the situation of a single electron in an otherwise empty conduction band at $T = 0$, when the local moment system is ferromagnetically saturated. In this case the Coulomb interaction is meaningless, the 'Hubbard function' $\Gamma_{ilm,j\sigma}(E)$ is identical to zero. In the zero-bandwidth limit, discussed in the last section, for the $\uparrow$-spectrum all spectral weights disappear except for $\alpha_{1\uparrow} = 1$, while for the $\downarrow$-spectrum the levels E_1 and E_2 survive with $\alpha_{1\downarrow} = \frac{1}{2S+1}$ and $\alpha_{2\downarrow} = \frac{2S}{2S+1}$.

For finite bandwidth the mentioned special case is that of a ferromagnetically saturated semiconductor [13, 14, 34–42]. In this case, the spin-$\uparrow$ quasiparticle density of states $\rho_\uparrow(E)$ is only rigidly shifted compared to the 'free' Bloch density of states:

$$\rho_\uparrow(E) \overset{T=0;n=0}{\longrightarrow} \rho_0(E + \tfrac{1}{2}JS). \tag{6}$$

Consequently, the quasiparticle dispersion is undeformed with respect to the Bloch energies, $E_\uparrow(\boldsymbol{k}) \to \epsilon(\boldsymbol{k}) - \frac{1}{2}JS$. The $\downarrow$-spectrum is more complicated because a $\downarrow$-electron has several possibilities to exchange its spin with the antiparallel f spins. Therefore, the $\sigma = \downarrow$-spinflip function is not at all trivial. However, its equation of motion decouples exactly, producing a closed system of equations which can be solved after Fourier transformation for the single-electron Green function. The corresponding self-energy $\Sigma_{\boldsymbol{k}\downarrow}(E)$ reads:

$$\Sigma_{\boldsymbol{k}\downarrow}(E) = \frac{1}{2}JS\left(1 + \frac{JB_{\boldsymbol{k}}(E)}{1 - \frac{1}{2}JB_{\boldsymbol{k}}(E)}\right) \tag{7}$$

$$B_{\boldsymbol{k}}(E) = \frac{\hbar}{N}\sum_{\boldsymbol{q}}\left(E - \epsilon(\boldsymbol{k}-\boldsymbol{q}) + \frac{1}{2}JS - \hbar\omega(\boldsymbol{q})\right)^{-1}. \tag{8}$$

$\hbar\omega(\boldsymbol{q})$ are the spin wave energies following from the Heisenberg exchange H_{ff} (cf equation (1)), $\hbar\omega(\boldsymbol{q}) = 2S(\hat{J}(\boldsymbol{q}=0) - \hat{J}(\boldsymbol{q}))$. $\hat{J}(\boldsymbol{q})$ is the Fourier transform of the exchange integral $\hat{J}_{ij}$. Usually the spin wave energies will be smaller by about two orders of magnitude

than other typical energies of the system such as the exchange constant J or the Bloch bandwidth W. As a general result the spectral density $S_{k\downarrow}(E)$ consists of two structures corresponding to special elementary excitation processes of the $\downarrow$ electron. There is a rather broad structure built up by 'scattering states' which result from magnon emission by the original $\downarrow$ electron. Thereby the excited electron reverses its spin becoming a $\uparrow$ electron. Such a process is possible only if there are $\uparrow$ band states within reach for the original $\downarrow$ electron to land after the spinflip. The scattering states therefore occupy the same energy region as the $\uparrow$-DOS (6).

There is another possibility for the $\downarrow$ electron to flip its spin. It can also be done by a repeated emission and reabsorption of a magnon by the conduction electron resulting in a 'dressed' particle propagating through the lattice accompanied by a virtual cloud of magnons. For not too small positive (negative) J the energy of this 'dressed' particle lies above (below)

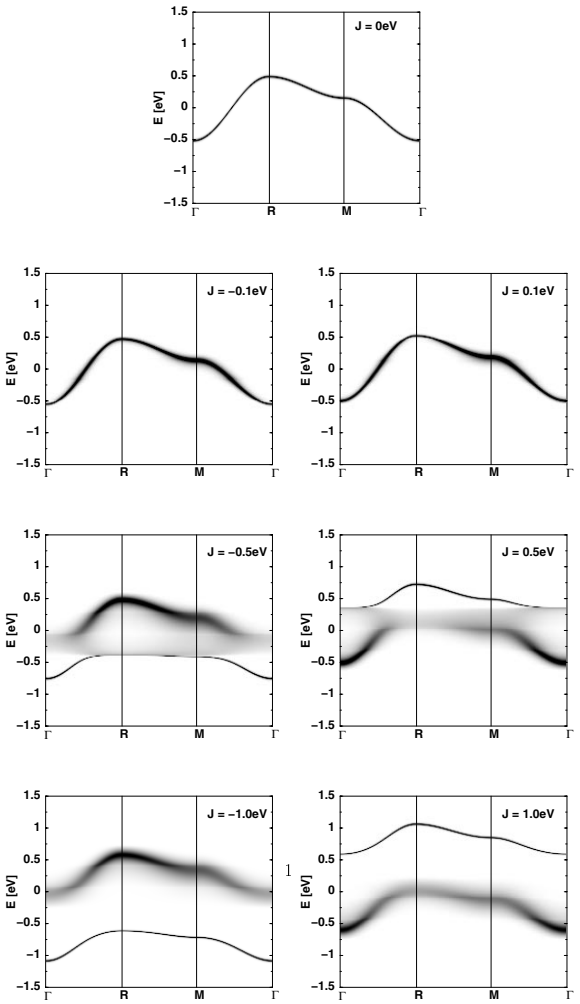

Figure 1. Spin-$\downarrow$ spectral densities (quasiparticle bandstructures) of the ferromagnetically saturated semiconductor for $S = \frac{1}{2}$ and J as indicated along several symmetry directions. The left (right) column displays the $J < 0$ ($J > 0$) case, the topmost picture shows the interaction-free spectral density.

the scattering spectrum giving even rise to a bound state, i.e. to a quasiparticle with infinite lifetime which we call the 'magnetic polaron'. Outside the scattering region the polaron peak manifests itself as a δ-function. As soon as the peak dips into the scattering part the polaron gets a finite lifetime after which it decays into a $\uparrow$ electron plus magnon. Figure 1 shows the down-spin quasiparticle bandstructure as derived from the respective spectral density as a density plot. The degree of blackening is a measure of the spectral density magnitude. Sharp dark lines refer to pronounced peaks in the spectral density representing quasiparticles with long lifetime. For weak coupling $|JS| < 0.1$ scattering processes smear out a little bit the 'free' dispersion but do not lead to strong deformations. However, already for moderate couplings $|JS| \gtrsim 0.2$ one recognizes for some $\boldsymbol{k}$ vectors the appearance of a sharp polaron dispersion. For $J > 0$ (right column) the magnetic polaron is stable on the high-energy side of the $\uparrow$ spectrum, for $J < 0$ on the low-energy side. In addition the scattering spectrum is clearly visible taking away a great part of the total spectral weight. In the antiferromagnetic KLM the magnetic polaron represents the ground state configuration [49]. For still rather moderate couplings of $|JS| \gtrsim 0.3$ the polaron dispersion has split off over the full Brillouin zone. The magnetic polaron has an infinite lifetime. It is surprising that even the broad scattering structure is obviously bunched together as if it were a rather stable quasiparticle. It is noteworthy to repeat that the results of figure 1 are exact and free of any uncontrollable approximation. So we have to also expect these quasiparticle effects in real systems. This holds also for the quasiparticle density of states (QDOS) plotted in figure 2 for several exchange couplings $|J|$. According to equation (6) the $\uparrow$-QDOS is only rigidly shifted to higher (lower) energies for $J < 0$ ($J > 0$). Correlation effects appear exclusively in the $\downarrow$ spectrum. For $|JS| \gtrsim 0.25$ a band splitting sets in. One of the subbands occupies the same energy region as $\rho_{\uparrow}(E)$ being therefore built up by the mentioned scattering states. In the ferromagnetic ($J > 0$) KLM it is the low energy part of the spectrum containing a considerable amount of $\downarrow$-spectral weight. This is not a specialty of

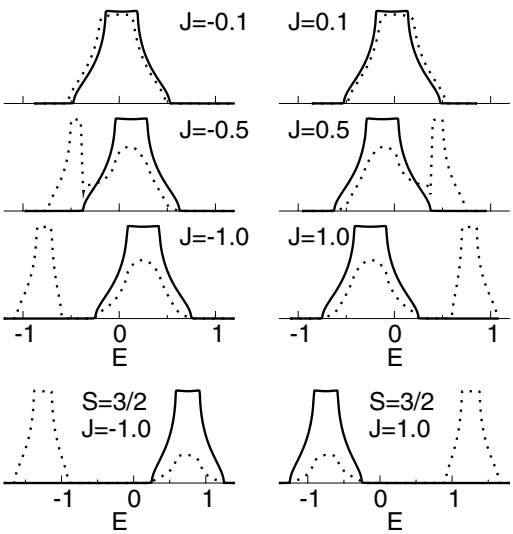

Figure 2. Spin-$\uparrow$ ($\downarrow$) density of states of the ferromagnetically saturated semiconducter as a function of energy plotted as a solid (dotted) line. The upper three figures of each column show the DOS for a $S = \frac{1}{2}$ system with interaction strengths $|J| \in \{0.1; 0.5; 1.0\}$ corresponding to the spectral densities of figure 1. The respective lowest figure shows a $S = \frac{3}{2}$ system with $|J| = 1.0$. The left (right) column corresponds to $J < 0$ ($J > 0$).

the $S = \frac{1}{2}$ case or of weak and moderate couplings exhibited in figure 2 but holds equivalently, e.g., for $S = \frac{3}{2}$ and in the strong coupling region ($|JS| \gtrsim 1.0$, see last row in figure 2). After the band splitting has set in the weights of the two spin-$\downarrow$ subbands are close to the zero-bandwidth values $\frac{1}{2S+1}$ for the lower, and $\frac{2S}{2S+1}$ for the upper part ($J > 0$), i.e. independent of J. The very often used assumption, when the KLM is applied to the manganites, that the e_g electron orients its spin parallel to the t_{2g} $S = \frac{3}{2}$ spin [25, 28], appears with respect to the exact results in figure 2 rather questionable. In the antiferromagnetic ($J < 0$) KLM the low energy quasiparticle subband consists of stable polaron states which build the high energy part in the ferromagnetic ($J > 0$) KLM. Although the $J > 0$ QDOS and the $J < 0$ QDOS appear as mirror-images the implied physics turns out to be rather different.

3. Dynamical mean-field theory

3.1. Mapping onto an impurity model

It is not possible to directly apply the methods of the dynamical mean-field theory [50] to the KLM. One exception is the case of the classical-spin limit ($S \to \infty$) [25, 26, 28], thus removing the quantum nature of the spins. The effect of quantum mechanics is strongest for $S = \frac{1}{2}$, but also for $S = \frac{7}{2}$ they dramatically influence the spectrum [13, 14]. The assumption of classical spins for $S = \frac{3}{2}$, as done in [25, 28], therefore needs careful analysis of the neglected effects.

Another possibility to derive a dynamical mean-field theory for the Kondo lattice model is the fermionization of the localized spin operators as suggested in [51]. This approach is, however, limited to $S = \frac{1}{2}$ systems (see also [52–54]). The first part of our approach will closely follow [51] but, as discussed below, will then differ from the cited reference.

The localized spins in the Hamiltonian (1) can be expressed in terms of auxiliary fermion operators $f_{i\sigma}$ ($f^{\dagger}_{i\sigma}$) [51]:

$$\boldsymbol{S}_i \to \boldsymbol{S}_i^{(f)} = \sum_{\sigma,\sigma'} f^{\dagger}_{i\sigma} \tau_{\sigma\sigma'} f_{i\sigma'}. \tag{9}$$

Here, $\tau_{\sigma\sigma'}$ represents the Pauli matrices. This is the same transformation that led to (2) where it was applied to the conduction electron spin σ_i. The 'fermionization' according to equation (9) implies the introduction of the constraint:

$$Q_i = \sum_{\sigma} n_{i\sigma}^{(f)} = \sum_{\sigma} f^{\dagger}_{i\sigma} f_{i\sigma} = 1 \quad \forall i. \tag{10}$$

The inclusion of this constraint via a Lagrange formalism corresponds to the addition of a Hubbard-like interaction term for the f-fermions to the Hamiltonian with the interaction constant $U^{(f)} \to \infty$ [51]. The one-particle energy of the f-fermions is located at $-\frac{U^{(f)}}{2}$. The 'fermionized KLM' takes the form:

$$H^{(\mathrm{ferm})} = \sum_{\boldsymbol{k},\sigma} \epsilon(\boldsymbol{k}) c^{\dagger}_{\boldsymbol{k}\sigma} c_{\boldsymbol{k}\sigma} - \frac{J}{2} \sum_{i} \sigma_i \cdot \boldsymbol{S}_i^{(f)} - \frac{U^{(f)}}{2} \sum_{i\sigma} f^{\dagger}_{i\sigma} f_{i\sigma} + \frac{U^{(f)}}{2} \sum_{i\sigma} n_{i\sigma}^{(f)} n_{i-\sigma}^{(f)}. \tag{11}$$

This Hamiltonian describes a system of two different kinds of $S = \frac{1}{2}$ fermions coupled by a local spin-exchange interaction. The f-fermions are additionally correlated via the Hubbard-type of interaction to prevent double occupancy. This Hamiltonian resembles the periodic Anderson model (PAM) [8] in some way. In fact the only difference in the operator structure is the 'coupling' between conduction band and f state. In the PAM, this is simply a kinetic-energy term ('hybridization'), whereas here, the two subsystems are coupled by the spin exchange. Essentially, the 'fermionized KLM' is a rudimentary version of the general multi-band Hubbard model with (local) inter-band interaction. For this model, the DMFT is discussed by [50]. It

is straightforward to apply the standard methods of the DMFT to map model (11) onto an appropriate impurity model with the corresponding self-consistency condition to determine the parameters of the impurity model. This leads to the following Hamiltonian for the impurity model (single-site Kondo model, SSKM) with fermionized f-spins:

$$H_{\mathrm{SSKM}}^{(\mathrm{ferm})} = \sum_{\boldsymbol{k},\sigma} \eta(\boldsymbol{k}) c_{\boldsymbol{k}\sigma}^{\dagger} c_{\boldsymbol{k}\sigma} - \frac{J}{2}\sigma_0 \cdot \boldsymbol{S}^{(f)} - \frac{U^{(f)}}{2}\sum_{\sigma} f_{\sigma}^{\dagger} f_{\sigma} + \frac{U^{(f)}}{2}\sum_{\sigma} n_{\sigma}^{(f)} n_{-\sigma}^{(f)} \tag{12}$$

with only one 'impurity' site for the f-fermions. The spin-exchange interaction acts only at this single site denoted by the site index 0. It is advisable to express the conduction band part of Hamiltonian (12) in local space and single out the operators referring to the impurity site 0:

$$\begin{aligned} \sum_{\boldsymbol{k},\sigma} \eta(\boldsymbol{k}) c_{\boldsymbol{k}\sigma}^{\dagger} c_{\boldsymbol{k}\sigma} &= \sum_{i,j,\sigma} T_{ij} c_{i\sigma}^{\dagger} c_{j\sigma} \\ &= \sum_{\sigma} T_{00} c_{0\sigma}^{\dagger} c_{0\sigma} + \sum_{\substack{i\neq 0 \\ \sigma}} T_{0i}\left(c_{0\sigma}^{\dagger} c_{i\sigma} + c_{i\sigma}^{\dagger} c_{0\sigma}\right) + \sum_{\substack{i,j\neq 0 \\ \sigma}} T_{ij} c_{i\sigma}^{\dagger} c_{j\sigma}. \end{aligned} \tag{13}$$

For better readability, we will denote the construction operators at the site 0 with the symbol d_{σ} ($d_{\sigma}^{\dagger}$), the on-site energy will be denoted $T_{00} \rightarrow e_d$. Finally we introduce a unitary transformation which diagonalizes the last term of the second line in equation (13). The transformed fermion operators will be denoted $a_{k\sigma}$ ($a_{k\sigma}^{\dagger}$), the hopping $T_{0i} \rightarrow V_{kd}$ and finally $T_{ij} \rightarrow \tilde{\eta}(k)$ for $i \neq j$. In the context of the DMFT, one does not need to know the explicit structure of this unitary transformation since $\tilde{\eta}(k)$ and V_{kd} need not be known explicitly either. The parameters of the single-site Kondo model will be determined by the self-consistency condition of the DMFT (see below).

A direct solution of model (12) is, to our knowledge not possible. However, it can be further simplified: the Hubbard term originating from the constraint (10) can be eliminated by simply reversing the 'fermionization' procedure which led from Hamiltonian (1) to (11). The auxiliary fermion operators get replaced by a local spin-$\frac{1}{2}$ operator at the impurity site, and the constraint (10) can be dropped. This leads to the final version of the single-site Kondo model:

$$H_{\mathrm{SSKM}} = \sum_{k,\sigma} \tilde{\eta}(k) a_{k\sigma}^{\dagger} a_{k\sigma} + e_d \sum_{\sigma} d_{\sigma}^{\dagger} d_{\sigma} + \sum_{k,\sigma} V_{kd}\left(d_{\sigma}^{\dagger} a_{k\sigma} + a_{k\sigma}^{\dagger} d_{\sigma}\right) - \frac{J}{2}\sigma^{(d)} \cdot \boldsymbol{S}. \tag{14}$$

This last step, which could be called 'de-fermionization', distinguishes our approach from the one used in [51] and elsewhere. This 'de-fermionization' ensures the exact fulfilment of the constraint (10), which could, for example, only be maintained on average ($\sum_{\sigma}\langle n_{\sigma}^{(f)}\rangle = 1$ instead of $\sum_{\sigma} n_{\sigma}^{(f)} = 1$) in [51].

The parameters determining the conduction band in the Hamiltonian (14), namely $\tilde{\eta}(k)$ and V_{kd}, have to be specified according to the DMFT self-consistency condition: the local conduction band Green function (cf (4)) should be equivalent to the d-operator Green function of the single-site model, $\langle\langle d_{\sigma}; d_{\sigma}^{\dagger}\rangle\rangle = G_{\sigma}^{(d)}(E)$:

$$\frac{1}{N}\sum_{\boldsymbol{k}} G_{\boldsymbol{k}\sigma}(E) = G_{\sigma}^{(d)}(E) = \frac{\hbar}{E - e_d - \Delta_{\sigma}(E) - \Sigma_{\sigma}^{(d)}(E)} \tag{15}$$

where the right-hand side follows from the formal solution of the equation of motion of $G_{\sigma}^{(d)}(E)$. So, instead of the usual definition for the hybridization function, $\Delta(E) = \sum_k \frac{V_{kd}^2}{E-\tilde{\eta}(k)}$, it has to be determined so that equation (15) holds. One will see below that the knowledge of $\Delta_{\sigma}(E)$, which can become spin-dependent through this procedure, is sufficient to solve the single-site Kondo model (14). Its dispersion $\tilde{\eta}(k)$ and the hybridization parameter V_{kd} need not to be determined explicitly.

The DMFT, i.e. the mapping of the KLM onto the single-site model, is, except for the limit of infinite spatial dimensions, an approximation, equivalent to the local approximation. In the exactly solvable case of the ferromagnetic semiconductor (cf section 2.3) this is equivalent to neglecting the magnon energies which are assumed to be at least one order of magnitude smaller than the energy scales under consideration here, e.g. bandwidth or J.

Next, we will introduce an approximative method to solve the single-site Kondo model defined by Hamiltonian (14) for an arbitrary hybridization function $\Delta_\sigma(E)$.

3.2. Hybridization approximation

In the following section, we derive an equation of motion-based method to solve the single-site Kondo model (14). Since in this section we deal only with this model, we suppress all subscripts distinguishing between quantities in the lattice and the single-site model.

The starting point is the equation of motion for the d-Green function:

$$E G_\sigma^{(d)}(E) = \hbar + e_d G_\sigma^{(d)}(E) + \sum_k V_{kd} \langle\langle a_{k\sigma}; d_\sigma^\dagger \rangle\rangle - \frac{J}{2} \sum_\sigma (z_\sigma I_\sigma(E) + F_\sigma(E)) \tag{16}$$

where the higher Green functions $I_\sigma(E) = \langle\langle d_\sigma S^z; d_\sigma^\dagger \rangle\rangle$ and $F_\sigma(E) = \langle\langle d_{-\sigma} S^{-\sigma}; d_\sigma^\dagger \rangle\rangle$, corresponding to the Green functions $I_{im,j\sigma}(E)$ and $F_{im,j\sigma}(E)$ for the lattice case, are introduced. The 'mixed' Green function $\langle\langle a_{k\sigma}; d_\sigma^\dagger \rangle\rangle$ can be eliminated by investigating its equation of motion:

$$\sum_k V_{kd} \langle\langle a_{k\sigma}; d_\sigma^\dagger \rangle\rangle = \sum_k \frac{V_{kd}^2}{E - \tilde{\eta}(k)} G_\sigma^{(d)}(E) = \Delta(E) G_\sigma^{(d)}(E) \tag{17}$$

thereby defining the hybridization function $\Delta(E) = \sum_k \frac{V_{kd}^2}{E - \tilde{\eta}(k)}$. This yields the final equation of motion:

$$(E - (e_d + \Delta(E))) \, G_\sigma^{(d)}(E) = \hbar - \frac{J}{2} \sum_\sigma (z_\sigma I_\sigma(E) + F_\sigma(E)) \, . \tag{18}$$

Equation (18) looks, except for the $\Delta(E)$ in the prefactor of $G_\sigma^{(d)}(E)$, like the equation of motion of the zero-bandwidth limit. The hybridization function $\Delta(E)$ is due to the V_{kd} term in the Hamiltonian (14). This term prohibits an exact solution. In fact, the 'hybridization' via V_{kd} is nothing else than the inter-site hopping which was neglected in the zero-bandwidth limit. This term will force us to make certain approximations in the determination of the higher Green functions on the right-hand side of equation (18). We will exemplify this using the $I_\sigma(E)$ function. Its equation of motion reads

$$\begin{aligned}(E - e_d) I_\sigma(E) &= \hbar \langle S^z \rangle + \sum_k V_{kd} \langle\langle a_{k\sigma} S^z; d_\sigma^\dagger \rangle\rangle - \frac{J}{2} \big(z_\sigma \langle\langle d_\sigma S^z S^z; d_\sigma^\dagger \rangle\rangle \\ &\quad + \langle\langle d_{-\sigma} S^{-\sigma} S^z; d_\sigma^\dagger \rangle\rangle - z_\sigma \langle\langle d_\sigma d_\sigma^\dagger d_{-\sigma} S^{-\sigma}; d_\sigma^\dagger \rangle\rangle \big)\end{aligned} \tag{19}$$

where on the one hand, higher 'impurity-site' Green functions are introduced, but on the other hand also a higher 'mixed' Green function, $\langle\langle a_{k\sigma} S^z; d_\sigma^\dagger \rangle\rangle$. In analogy to the one-particle mixed Green function, equation (17), we use the following substitution:

$$\sum_k V_{kd} \langle\langle a_{k\sigma} S^z; d_\sigma^\dagger \rangle\rangle \to \Delta(E) \langle\langle d_\sigma S^z; d_\sigma^\dagger \rangle\rangle = \Delta(E) I_\sigma(E). \tag{20}$$

The justification of this procedure can be found in analogy to the 'self-energy substitution' known from other approximation methods for the KLM (see e.g. [14]) by inspecting the spectral

representations of the relevant Green functions. This reveals that all of them have the same single-particle poles, they differ only in the respective weights given by matrix elements of the type $\langle E_n|A|E_m\rangle$. Here $|E_n\rangle$ are the energy eigenstates and A represents one of the relevant operators: d_σ, $a_{k\sigma}$, $d_\sigma S^z$ or $a_{k\sigma} S^z$. From equation (17) follows that the hybridization function accounts for the differences of the matrix elements of the first two operators (d_σ and $a_{k\sigma}$). Assuming that these differences are almost equal to those of the matrix elements built up by the latter two operators leads to the *hybridization approximation* (20).

This is the only approximation necessary to decouple the hierarchy of equations of motion. In the case of $S = \frac{1}{2}$ spins, there are only six different 'impurity-site' Green functions, whose equations of motion form a closed set of equations. Besides the already introduced Green functions $G_\sigma^{(d)}(E)$, $I_\sigma(E)$ and $F_\sigma(E)$, these are

$$\begin{aligned} F_\sigma^{(1)}(E) &= \langle\langle d_{-\sigma} d_{-\sigma}^\dagger d_\sigma S^z; d_\sigma^\dagger \rangle\rangle \\ F_\sigma^{(2)}(E) &= \langle\langle d_{-\sigma} d_\sigma^\dagger d_\sigma S^{-\sigma}; d_\sigma^\dagger \rangle\rangle \\ D_\sigma(E) &= \langle\langle d_{-\sigma} d_{-\sigma}^\dagger d_\sigma; d_\sigma^\dagger \rangle\rangle. \end{aligned} \tag{21}$$

Several expectation values, introduced into the theory via the inhomogeneities of the equations of motion, can be expressed in terms of the above-mentioned Green functions, a self-consistent solution has to be found.

At this point, let us comment on the reliability of this approximation. Although only one approximation enters our decoupling procedure (cf equation (20)), it still has to be seen as an uncontrollable approximation meaning that there is no true small parameter. There are two non-trivial limiting cases where the replacement (20) becomes exact: the first is the limit $V_{kd} \to 0$, representing the zero-bandwidth KLM of section 2.2. But already a small, but finite bandwidth in the KLM could lead to any (unknown) expression for $\Delta(E)$ implying that we can not necessarily assume V_{kd} to be small any more. The second limit is the 'classical spin' limit where the 'spin variable' S has no operator properties any more. Here, the replacement of equation (20) reduces to (17). However, since we are interested in the general case with finite S and bandwidth, we have to confirm the trustworthiness of this approximation by a comparison with other well-tested methods.

4. Other approximation methods

We are now going to introduce three further approximation methods for the KLM. These are known from the literature, their strengths and weaknesses have been identified. The three methods differ substantially with respect to the theoretical assumptions made for an approximate solution of the KLM. Common features following from these procedures and the above-introduced DMFT scheme should then give some credit of reliability, in particular when they additionally fit the exact limiting cases discussed in section 2.

4.1. Second-order perturbation theory

An application of the usual diagrammatic perturbation theory to the Kondo model cannot be performed due to the absence of Wick's theorem. Only for low temperatures (spin-wave approximation) [55] or in the classical-spin limit [56], is this method applicable. The projection operator formalism of Mori [43, 44] is better suited for the Kondo model. It has been used successfully to describe correlation effects in the Hubbard model in the weak coupling regime [57]. The general formula for the second-order contribution $\Sigma_{k\sigma}^{(2)}(E)$ can be found there (equation (3.12) in [57]). To allow for a better comparison with the other approximations in

this paper, we further approximate the self-energy taking only $\boldsymbol{k}$ averaged occupation numbers into account (local approximation).

4.2. Self-consistent CPA

Next, we want to introduce a modification of the well known 'coherent potential approximation' (CPA) [58] for the KLM. The CPA is a standard many-body approach that starts from a fictitious alloy in analogy to the interacting particle system. The starting point may be the zero bandwidth limit of section 2.2. We think of a four-component alloy each constituent of which is characterized by one of the energy levels E_i in equation (5). The spectral weights $\alpha_{i\sigma}$ (5) are then to be interpreted as the 'concentrations' of the alloy components as seen by a propagating σ-electron. The fictitious alloy for a σ-electron is built up by the local moments and by the frozen $(-\sigma)$ electrons. The CPA self-energy of the σ-electron is found by the well known formula [58]:

$$0 = \sum_{p=1}^{4} \alpha_{p\sigma} \frac{E_p - \Sigma_\sigma(E) - T_0}{1 - G_{ii\sigma}(E)(E_p - \Sigma_\sigma(E) - T_0)}. \tag{22}$$

As a consequence of the single-site aspect of the CPA the resulting self-energy is wave-vector independent. According to equation (5) the 'concentrations' $\alpha_{i\sigma}$ depend on a sum of the 'higher' correlation functions $I_{ii,i\sigma}(E)$ and $F_{ii,i\sigma}(E)$, which can rigorously be expressed by the single-electron Green function:

$$\gamma_\sigma + z_\sigma \Delta_\sigma = \frac{-1}{\hbar\pi} \frac{1}{N} \sum_{\boldsymbol{k}} \int_{-\infty}^{+\infty} \mathrm{d}E f_-(E)\,(E - \epsilon(\boldsymbol{k}))\,\mathrm{Im}G_{\boldsymbol{k}\sigma}(E). \tag{23}$$

The shortcomings of the CPA procedure lie to hand. One is the same as that in the conventional alloy analogy of the Hubbard model, namely the assumption of frozen $(-\sigma)$ electrons. This is partially removed by our proposed modification of the standard CPA procedure for the KLM, namely the self-consistent calculation of the higher correlation functions γ_σ and Δ_σ via equation (23) as well as the band occupation $\langle n_{-\sigma}\rangle$ via the spectral theorem for the one-electron Green function. Maybe even more serious in the case of the KLM is the blocking of repeated spin exchange with the local moment system. Magnon emission or absorption is not involved. So we cannot expect that the CPA treatment correctly reproduces the exact limiting case of section 2.3. However, some general information about the quasiparticle bandstructure might be possible, in particular in the strong coupling ('split band') regime. By construction the method yields the correct zero-bandwidth limit.

4.3. The moment-conserving decoupling approach (MCDA)

A Green function method which takes the spin dynamics correctly into account has been proposed in [14]. For details about this approach, we refer the reader to the cited paper, here we summarize the result briefly.

This decoupling approach yields finally a self-energy of the following form:

$$\Sigma_{\boldsymbol{k}\sigma}(E) = -\tfrac{1}{2} J z_\sigma \langle S^z\rangle + \tfrac{1}{4} J^2 D_{\boldsymbol{k}\sigma}(E). \tag{24}$$

The first term is linear in the coupling J and proportional to the 4f magnetization $\langle S^z\rangle$. It just represents the result of a mean-field approximation being correct in the weak-coupling limit. The second term in (24) contains all the spin exchange processes which may happen. It is a complicated functional of the self-energy itself. So (24) is not at all an analytical solution but an implicit equation for the self-energy. We do not present here the lengthy expression for $D_{\boldsymbol{k}\sigma}(E)$

referring the reader for further details to [14]. It should be mentioned, however, that $D_{k\sigma}(E)$ contains several expectation values which must be fixed to get a self-consistent solution. No problems arise with the mixed correlation functions $\gamma_\sigma = \langle S_i^\sigma c_{i-\sigma}^\dagger c_{i\sigma}\rangle$ and $\Delta_\sigma = \langle S_i^z n_{i\sigma}\rangle$. They can rigorously be expressed by the spin flip function $F_{ii,i\sigma}(E)$ and the Ising function $I_{ii,i\sigma}(E)$ defined previously. Both functions are already involved in the procedure, so that no further approximations are necessary to fix γ_σ and Δ_σ. For pure local-moment correlations such as $\langle S_i^z\rangle$, $\langle S_i^\pm S_i^\mp\rangle$,..., however, a special treatment is necessary, e.g. as described in [14].

5. Results

In this section, we discuss the results obtained for the DMFT and the three approximation schemes of section 4 for the ferromagnetic Kondo lattice model with $S = \frac{1}{2}$. Since we are interested in the reaction of the conduction band due to the magnetic order of the spin system, we have not calculated the latter self-consistently. Instead, we have simulated the magnetic order by determining $\langle S^z\rangle$ using a Brillouin function. Temperatures are given in units of T_c. Within the CPA, our choice of $\langle S^z\rangle$ can lead to unphysical results. Namely in the case of $\langle S^z\rangle \to S$, some of the weights (5) can become negative. There is an upper bound for $\langle S^z\rangle$ [33]. We therefore had to limit $\langle S^z\rangle$ to $\langle S^z\rangle \lesssim 0.33$ for some of the CPA calculations. Within the DMFT calculations, we experienced severe numerical problems which forced us to introduce a further approximation: 'mean-field'-decoupling the $F_\sigma^{(1)}(E)$ and $F_\sigma^{(2)}(E)$ functions simplifies the system of equations of motion:

$$\begin{aligned} F_\sigma^{(1)}(E) &\approx (1 - \langle n_{-\sigma}\rangle)\Gamma_\sigma(E) + \langle S^z\rangle D_\sigma(E) + \langle (1 - n_{-\sigma})S^z\rangle G_\sigma^{(d)}(E) \\ F_\sigma^{(2)}(E) &\approx \langle n_\sigma\rangle F_\sigma(E) - \langle S^{-\sigma} d_\sigma^\dagger d_{-\sigma}\rangle G_\sigma^{(d)}(E). \end{aligned} \tag{25}$$

All DMFT results presented below were obtained using the hybridization approximation in combination with this unrestricted-mean-field decoupling of $F_\sigma^{(1)}(E)$ and $F_\sigma^{(2)}(E)$.

In all calculations, the conduction band is described by a tight-binding DOS for a simple-cubic lattice structure [59] of unit width ($W = 1$ eV). The Curie temperature is taken as $T_c = 250$ K.

The quasiparticle densities of states (DOS) for quarter-filling and different values of J are plotted in figures 3 and 4 for $T = 0$ and $T = T_c$, respectively. As indicated, the columns correspond to DMFT, MCDA, CPA and SOPT, respectively (from left to right).

We will begin the discussion with the DMFT results shown in the left column of figure 3. A small value of J leads to a spin-dependent shift of the spin-↑ and -↓ DOS, as one would obtain by a simple mean-field decoupling, i.e. by replacing S^z by its mean value $\langle S^z\rangle$ in Hamiltonian (1). With increasing J, the DOS show some striking correlation effects: first a broadening, later the onset of a splitting of the band can be observed. Whereas, in general, the correlation effects are stronger for spin ↓ (indicated by a stronger quasiparticle damping), the splitting is, in contrast to the other two methods, more pronounced in the spin-↑ DOS. However, here the split-off (upper) peak has much less spectral weight than the original peak which, except for a band-narrowing, still resembles strongly the free conduction band DOS.

The picture is very similar in the MCDA. Again, a mean-field-like spin-dependent bandshift is observed for small J. On increasing J, the spin-↓ DOS broadens, and a two-peak structure emerges. The spin-↑ DOS remains, except for a small tail at its upper edge, unchanged. This behaviour can easily be understood by comparing with the special case of the ferromagnetically saturated semiconductor as discussed in section 2.3, since the MCDA develops continuously into this special case for $n \to 0$ and $T \to 0$. The spin-↓ DOS splits into a scattering part (low energies) and the polaron-like part at higher energies above the conduction band. Unlike the $n = 0$ case, however, there is some, though only weak, modification in the ↑

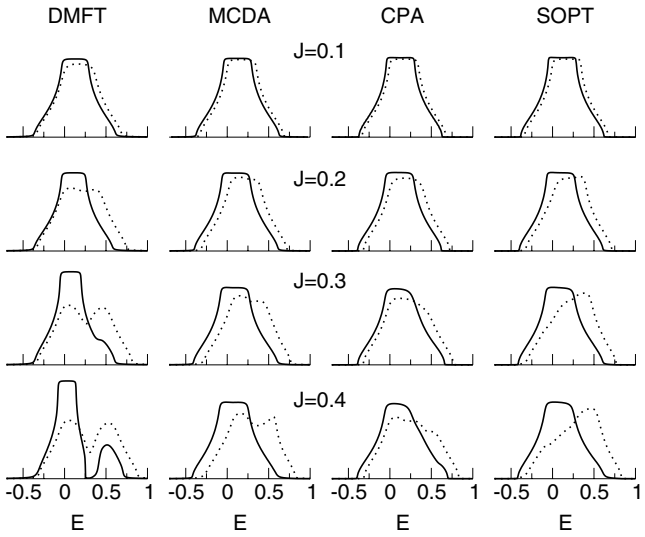

Figure 3. Conduction band density of states (DOS) obtained via the DMFT, MCDA, CPA and SOPT (from left to right) for different values of J as function of energy. The temperature is set to $T = 0$, therefore $\langle S^z \rangle = 0.5$ (CPA: $\langle S^z \rangle = 0.33$, see text) and the electron density $n = 0.5$, the chemical potential is at $\mu = 0$. Full curve, spin-$\uparrow$; dotted curve, spin-$\downarrow$ DOS.

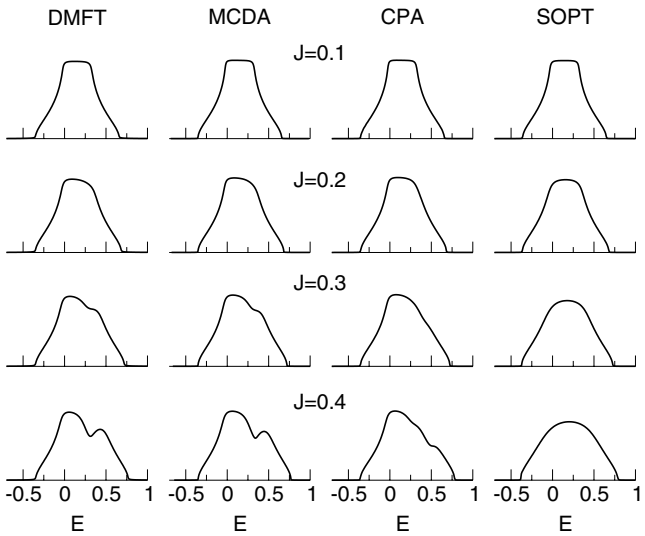

Figure 4. Same as figure 3, but for $T = T_c$, therefore $\langle S^z \rangle = 0$.

DOS, namely the above mentioned tail at its upper edge. This can be interpreted as a scattering contribution for spin-$\uparrow$ electrons. The origin of this is the finite number of spin-$\downarrow$ electrons.

Also the CPA DOS show a remarkably similar picture to the previously discussed theories. Again, there is the mean-field shift for small J. For larger values of J, the splitting of the spin-$\downarrow$ DOS sets in similarly to the other two methods. Here, this can be attributed to the two single-occupancy quasiparticle energies E_1 and E_2 known from the zero-bandwidth limit (cf section 2.2). For $n \neq 0$ a third quasiparticle energy carries non-vanishing weight, namely the

E_4 peak. This is located between the two other peaks since we switched off the conduction band Coulomb interaction U (cf equation (1)). For $J = 0.4$, the appearance of this third peak in between the two main peaks is vaguely visible. A remarkable difference from the DMFT and MCDA results is the fact, that the spin-$\uparrow$ and scattering part of the spin-$\downarrow$ DOS do not cover the same energy range. This shortcoming of the CPA is due to the neglect of spin-dynamics (magnons) as mentioned in section 4.2 (cf [40]).

The SOPT results are, for the plotted values of J in the weak- and intermediate-coupling regime, not too far away from the other results. For small J, where the SOPT becomes by definition reliable, the mean-field shift as in the other methods is clearly observable. Similar to the other methods, the deformation of the spin-$\downarrow$ DOS is much stronger than that of the spin-$\uparrow$ DOS. However, for larger J, the SOPT never shows a true band splitting, its range of validity is certainly restricted.

For $T = T_c$, where spin-symmetry is re-established, the DMFT, MCDA and CPA give a similar overall picture. The resulting DOS shows, already for $J \gtrsim 0.3$, a two-peak structure (DMFT and MCDA), in the CPA a third peak is faintly noticeable. The most remarkable observation is the near-coincidence of the DMFT and MCDA results for all J values. The transition from the (clearly distinct) $T = 0$ DOS to the (resembling) $T = T_c$ DOS is continuous for both theories. The SOPT, however, has to be seen as a complete failure for a paramagnetic system already for relatively small $J \approx 0.3$. This can already be read from the formula for calculating the self-energy, which is more or less trivial. The corresponding results cannot be connected to any of the exactly solvable limiting cases (cf section 4.1).

A firm-standing interpretation of the observations is not difficult since the MCDA can be traced back to the exactly solved limiting case of the ferromagnetically saturated semiconductor (cf section 2.3) and the CPA to that of the zero-bandwidth limit discussed in section 2.2. The SOPT, of course, becomes reliable for small J. Although all four presented methods are of approximate nature and their results do, at least for intermediate-to-large values of J, differ, some common properties emerge. For small J, the behaviour is genuine mean-field like, a bandshift proportional to $\pm J\langle S^z\rangle$ is observed. For larger J, the onset of a band splitting occurs. At $T = 0$ this primarily affects the spin-$\downarrow$ DOS. This fact is understandable by examination of the ferromagnetically saturated semiconductor where the band splitting was discussed in terms of a scattering band and the magnetic polaron. In that case the spin-$\uparrow$ DOS remains, except for a simple shift, unaffected by the interaction simply because spin-flip of spin-$\uparrow$ electrons is suppressed in this case. Now for finite n, this is only approximately true. The spin-$\downarrow$ DOS still shows strong correlation effects, but also the spin-$\uparrow$ DOS is affected due to the finite number of spin-$\downarrow$ electrons in the system. This manifests itself differently in the various methods: in the MCDA, a tail is seen at the upper edge of the spin-$\uparrow$ DOS; in the CPA, a shoulder develops; and in the DMFT approach, a band splitting is observable. From this we conclude that correlation effects are much more pronounced in the DMFT than in the other two theories. At $T = T_c$, the dip indicating the onset of the band splitting still exists for all but the SOPT method. In the CPA, MCDA and DMFT results this splitting is of similar size, which can easily be read off the CPA where it is simply given by the difference of the respective energies from the zero-bandwidth limit (see equation (5)). The two most pronounced peaks correspond to the single-occupancy quasiparticle energies E_1 and E_2, the band splitting is therefore approximately $\Delta E = J(S + \frac{1}{2})$.

This is in contrast to the results obtained by dynamical mean-field theory for the $S \to \infty$ KLM (KLM with classical spins). The emerging picture for classical spins is the following [26]: At $T = 0$, the DOS is characterized by a mean-field-like 'Zeeman' splitting between the bands of both spin directions. With increasing temperature, at each of the respective spin-$\uparrow$ or -$\downarrow$ bands, spectral weight of the opposite spin direction appears, until finally at $T = T_c$, the

system becomes paramagnetic. The splitting into two subbands separated by $\Delta E = JS$ stays constant. Comparing our results with the $S \to \infty$ ones, phenomenologically the DOSs show completely different characteristics at $T = 0$, especially in the spin-$\downarrow$ band. For $T = T_c$, the DOSs look quite similar. However, the physics behind the scenes turns out to be completely different as can be seen, e.g., by the inconsistent size of the band splitting ΔE. Whereas in the classical-spin limit, the splitting is always due to a mean-field-like 'on-site Zeeman splitting', in the case of quantum spins, the various elementary excitations, as discussed in the case of the ferromagnetically saturated semiconductor, are responsible for the sub-band structure. For the ferromagnetically saturated system, the neglect of spin-flip processes and magnons in the $S \to \infty$ calculation lead to the picture of a half-metal [26]. This does not apply for any finite value of S and is therefore clearly an artifact of the $S \to \infty$ limit.

Let us briefly remark on the situation with anti-ferromagnetic coupling ($J < 0$) [60]. All four approximation methods presented here do not show any signs of Kondo screening. An investigation of the special low-temperature physics of the model with $J < 0$ is therefore not possible. However, some remarks about the behaviour of the model for $T > T_K$ can be made: In general the excitation spectra are broader than in the $J > 0$ case. The resulting exchange splitting of $\Delta E \approx J(S + 1)$ is also larger than for $J > 0$ which can already be seen in the zero-bandwidth limit. This is again in sharp contrast to the $S = \infty$ results, where the size of the splitting is independent of the sign of J.

6. Conclusions

In this paper, we investigated the Kondo lattice model (KLM) focusing on the model with positive (ferromagnetic) exchange constant J. We discussed two exactly solvable, but nevertheless non-trivial limiting cases as well as four different approximation methods. The results obtained by these methods, maybe except for the perturbation theory, compare generally reasonably well. Sometimes even nearly perfect matches occur (cf figure 4). In general, the differences between the methods are smaller for the paramagnetic than the ferromagnetic system.

From the comparison of common features of these approximation methods in combination with the exact results, the following picture emerges for the quasiparticle structure of the ferromagnetic Kondo lattice model. For small $|J|$, a mean-field-like shift of $\uparrow$ and $\downarrow$ DOS is visible. Already for intermediate coupling strengths, a band splitting of size $\Delta E = J(S + \frac{1}{2})$ occurs. The relevant energy scale for the splitting is $JS \approx 0.3$. In the case of ferromagnetic saturation ($T = 0$), the splitting is more pronounced in the $\downarrow$ than in the $\uparrow$ DOS. This band-splitting should not be confused with the splitting found in the limit of 'classical spins' ($S \to \infty$). There, the splitting is simply due to a mean-field-like Zeeman splitting and therefore of the size $\Delta E = JS$. Contrary to that, our results clearly show that the two emerging subbands can be traced back to the two elementary excitations known from the limit of the ferromagnetically saturated semiconductor (see above). The magnetic saturation of the spin-system suppresses these processes for spin-$\uparrow$ electrons which explains the stronger footprint of the correlations in the spin-$\downarrow$ DOS. For finite temperatures, the magnetic polaron generally remains a well defined quasiparticle, represented by a rather sharp Lorentzian peak in the spectral density. Now the spin-$\uparrow$ electrons can also participate in spin-exchange processes since the localized spins are not fully aligned any more. The spin-symmetric DOS at $T \gtrsim T_c$ also show the characteristic splitting. Our results also confirm the fundamental differences between the $J > 0$ and $J < 0$ cases of the Kondo lattice model. It can be seen that both exactly solvable limiting cases that the ground state will be different depending on the sign of J. The approximative approaches of sections 3 and 4 do not allow a deeper investigation of

the model with $J < 0$ due to the inability to reproduce the special low-temperature properties of that model ('Kondo physics'). Another important conclusion from our calculations can be drawn: there is always finite spin-$\downarrow$ spectral weight in the region of the spin-$\uparrow$ DOS. This spectral weight does not disappear in the limit $J \to \infty$ but only in the limit $S \to \infty$ ('classical spins'). For the ferromagnetic KLM ($J > 0$), this implies that the KLM for $S = \frac{3}{2}$ and large J, corresponding to the situation found in manganites, will not be a half-metal for $T = 0$, contrary to the predictions of $S \to \infty$ calculations.

Acknowledgments

Financial support by the Volkswagen-Foundation within the project 'Phasendiagramm des Kondo-Gitter-Modells' is gratefully acknowledged. This work also benefitted from the financial support of the Sonderforschungsbereich SFB 290 ('Metallische dünne Schichten: Struktur, Magnetismus und elektronische Eigenschaften') of the Deutsche Forschungsgemeinschaft. One of us (DM) would like to thank the Friedrich-Naumann-Foundation for supporting his work.

References

[1] Zener C 1951 *Phys. Rev.* **81** 440
[2] Anderson P W and Hasegawa H 1955 *Phys. Rev.* **100** 675
[3] Kasuya T 1956 *Prog. Theor. Phys.* **16** 45
[4] Kondo J 1964 *Prog. Theor. Phys* **32** 37
[5] Nagaev E L 1974 *Phys. Status Solidi* b **65** 11
[6] Nolting W 1979 *Phys. Status Solidi* b **96** 11
[7] Anderson P W 1961 *Phys. Rev.* **124** 41
[8] Hewson A C 1993 *The Kondo Problem to Heavy Fermions* (Cambridge: Cambridge University Press)
[9] Schrieffer J R and Wolff P A 1966 *Phys. Rev.* **149** 491
[10] Wachter P 1979 *Handbook on the Physics and Chemistry of Rare Earth* vol 2, ed K A Gschneidner and L Eyring (Amsterdam: Elsevier) p 507
[11] Kossut J 1976 *Phys. Status Solidi* b **78** 537
[12] Legfold S 1980 *Ferromagnetic Materials* vol 1, ed E P Wohlfarth (Amsterdam: North-Holland) chapter 3
[13] Nolting W, Mathi Jaya S and Rex S 1996 *Phys. Rev.* B **54** 14455
[14] Nolting W, Rex S and Mathi Jaya S 1997 *J. Phys.: Condens. Matter* **9** 1301
[15] Rex S, Eyert V and Nolting W 1999 *J. Magn. Magn. Mater.* **192** 529
[16] Jin S, Tiefel T H, McCormack M, Fastnacht R A, Ramesh R and Chen L H 1994 *Science* **264** 413
[17] Ramirez A P 1997 *J. Phys.: Condens. Matter* **9** 8171
[18] Dagotto E, Yunoki S, Malvezzi A L, Moreo A, Hu J, Capponi S, Poilblanc D and Furukawa N 1998 *Phys. Rev.* B **58** 6414
[19] Satpathy S, Popović Z S and Vukajlović F R 1996 *Phys. Rev. Lett.* **76** 960
[20] Pickett W and Singh D J 1996 *Phys. Rev.* B **53** 1146
[21] Singh D J and Pickett W E 1998 *Phys. Rev.* B **57** 88
[22] Park J-H, Chen C T, Cheong S-W, Bao W, Meigs G, Chakarian V and Idzerda Y U 1996 *Phys. Rev. Lett.* **76** 4215
[23] Saitoh T, Sekiyama A, Kobayashi K, Mizokawa T, Fujimori A, Sarma D D, Takeda Y and Takano M 1997 *Phys. Rev.* B **56** 8836
[24] Okimoto Y, Katsufuji T, Ishikawa T, Urushibara A, Arima T and Tokura Y 1995 *Phys. Rev. Lett.* **75** 109
[25] Millis A J, Mueller R and Shraiman B I 1996 *Phys. Rev.* B **54** 5405
[26] Furukawa N 1999 *Physics of Manganites* ed T A Kaplan and S D Mahanti (New York: Plenum) p 1
[27] Millis A J, Littlewood P B and Shraiman B I 1995 *Phys. Rev. Lett.* **74** 5144
[28] Held K and Vollhardt D 2000 *Phys. Rev. Lett.* **84** 5168
[29] Chattopadhyay A, Millis A J and Das Sarma S 2000 *Preprint* cond-mat/0004151
[30] Singh R R P, Pickett W E, Hone D W and Scalapino D J 2000 *Comment. Mod. Phys.* **2** (1) B1
[31] Zhao G-M and Keller H 2000 *Preprint* cond-mat/0008151
[32] Saitoh T, Dessau D S, Moritomo Y, Kimura T, Tokura Y and Hamada N 2000 *Phys. Rev.* B **62** 1039

[33] Nolting W and Matlak M 1984 *Phys. Status Solidi* b **123** 155
[34] Methfessel S and Mattis D C 1968 *Handb. Phys.* **18** 389
[35] Izyumov Y A and Medvedev M V 1971 *Sov. Phys.–JETP* **32** 302
[36] Richmond P 1970 *J. Phys. C: Solid State Phys.* **3** 2402
[37] Shastry B S and Mattis D C 1981 *Phys. Rev.* B **24** 5340
[38] Allan S R and Edwards D M 1982 *J. Phys. C: Solid State Phys.* **15** 2151
[39] Auslender M I, Irkhin V Yu and Katsnelson M I 1984 *J. Phys. C: Solid State Phys.* **17** 669
[40] Auslender M I and Irkhin V Yu 1985 *J. Phys. C: Solid State Phys.* **18** 3533
[41] Nolting W, Dubil U and Matlak M 1985 *J. Phys. C: Solid State Phys.* **18** 3687
[42] Nolting W and Dubil U 1985 *Phys. Status Solidi* b **130** 561
[43] Mori H 1965 *Prog. Theor. Phys.* **33** 423
[44] Mori H 1966 *Prog. Theor. Phys.* **34** 399
[45] Kubo K 1974 *J. Phys. Soc. Japan* **36** 32
[46] Nolting W 1997 *Viel-Teilchen-Theorie (Grundkurs: Theoretische Physik 7)* 4th edn (Braunschweig: Vieweg)
[47] Edwards D M, Green A C M and Kubo K 1999 *J. Phys.: Condens. Matter* **11** 2791
[48] Green A C M and Edwards D M 1999 *J. Phys.: Condens. Matter* **11** 10511
[49] Tsunetsugu H, Sigrist M and Ueda K 1997 *Rev. Mod. Phys.* **69** 809
[50] Georges A, Kotliar G, Krauth W and Rozenberg M J 1996 *Rev. Mod. Phys.* **68** 13
[51] Matsumoto N and Ohkawa F 1995 *Phys. Rev.* B **51** 4110
[52] Pruschke T, Steininger B and Keller J 1995 *Physica* B **206–207** 154
[53] Jarrell M, Pang H, Cox D L and Luk K H 1996 *Phys. Rev. Lett.* **77** 1612
[54] Schork T, Blawid S and Igarashi J 1999 *Phys. Rev.* B **59** 9888
[55] Woolsey R B and White R M 1970 *Phys. Rev.* B **1** 4474
[56] Rys F, Helman J and Baltensperger W 1967 *Phys. Kondens. Materie* **6** 105
[57] Bulk G and Jelitto R J 1990 *Phys. Rev.* B **41** 413
[58] Velický B, Kirkpatrick S and Ehrenreich H 1968 *Phys. Rev.* **175** 747
[59] Jelitto R J 1969 *J. Phys. Chem. Solids* **30** 609
[60] Meyer D 2001 Electron correlation effects in ferromagnetic local-moment and intermediate-valence systems *Dissertation* Humboldt-Universität zu Berlin